

ESTIMATION OF STRESS INTENSITY FACTORS BY SIGMA PROCEDURE

M. C. Munwam

Graduate School of Science and Technology, Kumamoto University,
Kumamoto, Japan

M. Ohtsu

Department of Civil Engineering and Architecture, Kumamoto University,
Kumamoto, Japan

H. P. Rossmatith

Institute of Mechanics, Vienna University of Technology, Vienna, Austria

Abstract

Numerous workers have employed fracture mechanics concepts in order to improve the understanding of mechanical failure modes in concrete structures. A moment tensor analysis (SiGMA) of acoustic emission (AE) can provide quantitative information on cracking mechanisms. A relation between the moment tensor components and the stress intensity factors is derived. In bending tests of notched concrete beams, the direction of nucleated crack is determined by the SiGMA procedure. Based on the maximum circumferential stress criterion, the normalized stress intensity factors for mixed-mode cracking are estimated from the eigenvectors of the moment tensors.

Key words: Mixed-mode Fracture, Moment tensor analysis of acoustic emission (AE), Normalized stress intensity factors.

1 Introduction

The theory of AE wave motions was generalized on the basis of elastodynamics and dislocation theory (Ohtsu and Ono, 1984). Crack kinematics of AE source can be determined by the crack motion vector (Burgers vector) and the unit vector normal to the crack plane, which lead to the moment tensor. Earlier, the moment tensor analysis was employed

in studying glass failure due to indentation (Kim and Sachse, 1984). Based on an eigenvalue analysis of the moment tensor components, the classification of the type of crack and the determination of crack orientation were performed by the SiGMA (Simplified Green's Functions for Moment Tensor Analysis) procedure (Ohtsu, 1991). The analysis was also successfully applied to fracture tests of concrete specimens (Suaris and Van Mier, 1995).

Since the first application of linear elastic fracture mechanics concepts to concrete (Kaplan, 1961), numerous workers have employed the Griffith-Irwin (1920, 1958) fracture ideas in order to investigate the modes of mechanical failure in concrete. It is found that the inelastic zone (fracture process zone) requires the use of non-linear fracture mechanics for quasi-brittle materials such as concrete and cementitious materials. Still, a fictitious critical stress intensity factor (K_{IC}) can be defined as a material property by means of a suitable fracture criterion. For mixed-mode cracking the maximum circumferential stress criterion (Erdogan and Sih, 1963) has been employed for crack growth predictions in concrete (Chahrour and Ohtsu, 1994). Based on the relation between the direction of crack extension and the stress intensity factors from the maximum circumferential stress concept, the crack orientation obtained from the SiGMA procedure is applied to estimate the normalized stress intensity factors, $K_I^* = K_I/K_{IC}$ and $K_{II}^* = K_{II}/K_{IC}$.

2 Moment tensor analysis

Crack kinematics of AE source is modeled by crack motion vector (Burgers vector), \mathbf{b} , and normal vector, \mathbf{n} . The crack vector \mathbf{b} (\mathbf{y} , t) is decomposed into the direction vector \mathbf{l} and the amplitude of crack motion b (\mathbf{y} , t). Apart from the kinetic effect, kinematics of source characteristics are represented by an equivalent tensor as follows:

$$\int_F C_{pqkl} [b(y)l_k] n_l ds = [C_{pqkl} l_k n_l] \left[\int_F b(y) ds \right] = [C_{pqkl} l_k n_l] \Delta V = m_{pq}, \quad (1)$$

where C_{pqkl} are the elastic constants and ΔV is the crack volume. In an isotropic material, the moment tensor, m_{pq} , can be represented as follows:

$$m_{pq} = [C_{pqkl} l_k n_l] \Delta V = \begin{pmatrix} \lambda_k n_k + 2\mu l_1 n_1 & \mu l_1 n_2 + \mu l_2 n_1 & \mu l_1 n_3 + \mu l_3 n_1 \\ \mu l_2 n_1 + \mu l_1 n_2 & \lambda_k n_k + 2\mu l_2 n_2 & \mu l_2 n_3 + \mu l_3 n_2 \\ \mu l_3 n_1 + \mu l_1 n_3 & \mu l_3 n_2 + \mu l_2 n_3 & \lambda_k n_k + 2\mu l_3 n_3 \end{pmatrix} \Delta V \quad (2)$$

where λ and μ are Lamé's constants, and the scalar product $l_k n_k$ obeys

the summation convention.

3 Maximum circumferential stress criterion

In the case of mixed-mode fracture, a criterion for crack extension based on the linear elastic fracture mechanics (LEFM) was proposed by Erdogan and Sih (1963). The direction of crack extension θ is determined as the direction of maximum circumferential stress. Extension of the crack is governed by the critical stress intensity factor, K_{IC} , which follows from,

$$\cos \frac{\theta}{2} \left[K_I \cos^2 \frac{\theta}{2} - \frac{3}{2} K_{II} \sin \theta \right] = K_{IC}, \quad (3)$$

$$K_I \sin \theta + K_{II} (3 \cos \theta - 1) = 0. \quad (4)$$

Once a crack has nucleated, the crack vectors l and n are prescribed as given in Fig. 1. Thus, the direction of vector n is known to be equivalent to $(\cos(\theta + \pi/2), \sin(\theta + \pi/2))$. The orientations of l and n are readily obtained from the eigenvectors of moment tensor components. Three eigenvectors are determined from Eq.2. In the SiGMA procedure, unit vectors \bar{e}_1 , \bar{e}_2 and \bar{e}_3 , of directions $l + n$, $l \times n$ and $l - n$, are determined, respectively.

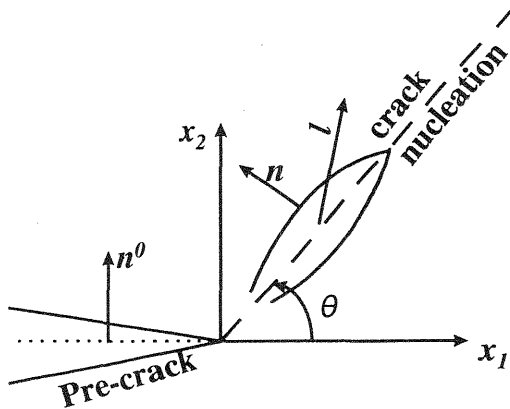


Fig. 1 Direction of crack extension and crack normal

Normalized stress intensity factors K_I^* and K_{II}^* can be determined from Eqs.3 and 4, as follows:

$$K_I^* = K_I / K_{IC} = \frac{3 \cos \theta - 1}{\cos \frac{\theta}{2} (1 + \cos \theta)}, \quad (5)$$

$$K_{II}^* = K_{II} / K_{IC} = \frac{-\sin \theta}{\cos \frac{\theta}{2} (1 + \cos \theta)}. \quad (6)$$

In order to relate Eqs.5 and 6 with the crack normal \mathbf{n} in Fig. 1, the coordinate system is transformed and two new vectors \mathbf{l}^* and \mathbf{n}^* are defined by,

$$\begin{aligned} \mathbf{l}^* &= \frac{\sqrt{2+2l_k n_k} \vec{e}_1^* + \sqrt{2-2l_k n_k} \vec{e}_2^*}{2}, \\ \mathbf{n}^* &= \frac{\sqrt{2+2l_k n_k} \vec{e}_1^* - \sqrt{2-2l_k n_k} \vec{e}_2^*}{2} \end{aligned} \quad (7)$$

where \vec{e}_1^* and \vec{e}_2^* are the transformed vectors of \vec{e}_1 and \vec{e}_3 , respectively. Setting $\mathbf{n}^* = (-\sin \theta, \cos \theta)$, the normalized stress intensity factors can be estimated from Eqs.5 and 6

4 Experiments

4.1 Specimens and fracture test

Concrete and mortar specimens of dimensions 10 cm x 10 cm x 40 cm were made and moisture-cured for 28 days in the standard room (20°C). Mechanical properties of specimens, obtained from cylindrical samples of 10 cm in diameter and 20 cm in height, are summarized in Table 1.

Table 1. Mechanical properties of specimens

	Compressive strength	Tensile strength	Poisson ratio	Young's modulus	P-wave velocity
	(MPa)	(MPa)		(GPa)	(m/s)
concrete	52.8	4.12	0.24	32.5	4730
mortar	53.7	2.93	0.19	23.4	4130

Tests of three-point bending were conducted in CC type (center notch, center loading), OC type (off-center notch, center loading), CO type (center notch, off-center loading). At the age of 28 days, a sawed pre-

cracked notch of 3 cm depth and 1 mm width was introduced in each specimen. The experimental set-up and AE sensor locations are shown in Fig. 2. Six AE sensors are arranged to cover the fracture process zone formed ahead of the notch. Sensors denoted by solid symbols are attached to the front, bottom and top surface. The others (blank symbols) are located on the back surface. Locations of one-point loading and notch are indicated by solid lines for center and by broken lines for off-center. Specimens of the CC type were prepared to form the fracture process zone under mode-I cracking. Mixed-mode cracking was expected in the specimens of the OC and the CO types. Loading speed of 0.01 mm/min was applied to specimens of the CC type, whereas loading speed applied to specimens of the OC and the CO types was 0.02 mm/min. This is because crack extension of the CC type was faster than that of the OC and the CO types. Inserting a clip gauge into the notch, the crack-mouth opening displacement (CMOD) could also be measured.

4.2 AE measurement and data analysis

AE sensors of 150 kHz resonant frequency have been employed. The amplification is 60 dB gain, and the frequency range is 200 kHz-1 MHz. AE waveforms were detected, amplified, filtered, and recorded by using LOCAN-TRA system (PAC). After the tests, two waveform-parameters of the arrival time and the amplitude of the first motion were read from the recorded waveforms, by displaying on the CRT screen. Then, the AE sources locations and the moment tensor components were determined by the SiGMA procedure. AE sources of which the shear ratios were smaller than 40% were classified as tensile cracks, while the AE sources with shear ratios greater than 60% were classified as shear cracks. AE sources of the shear ratios between 40% and 60% were referred to as mixed-mode.

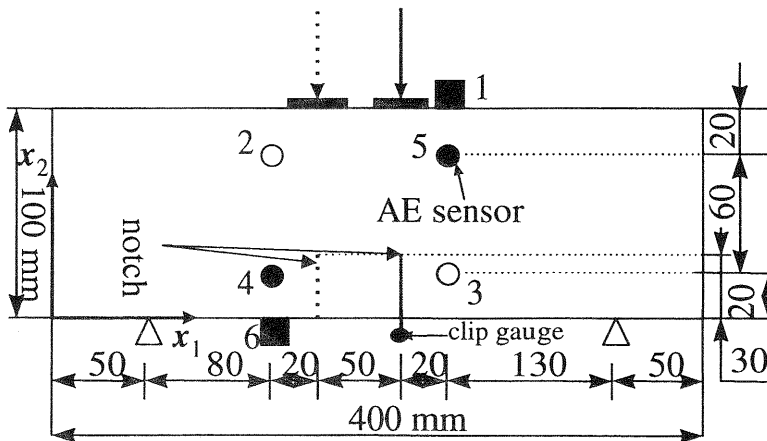


Fig. 2. Experimental set-up

A post-analysis (Ohtsu, 1995) was conducted. Theoretical AE waveforms at AE sensor locations were synthesized, by substituting AE source location and the moment tensor components. The two parameters of each theoretical waveform were automatically read and the SiGMA procedure was applied again. AE sources giving rise to crack kinematics in the post-SiGMA which were in good agreement with those of the previous SiGMA analysis were chosen as reliable solutions.

5 Results and discussion

5.1 SiGMA analysis

After the post analysis, cracks classified according to section 4.2 were plotted at their locations. Some results are shown in Fig. 3. For each crack two lines indicate the directions of either crack normal n or crack motion l . Only in the case of tensile cracks, lines with arrow symbols are employed. Thus, crack kinematics in the fracture process zone is determined by the SiGMA procedure.

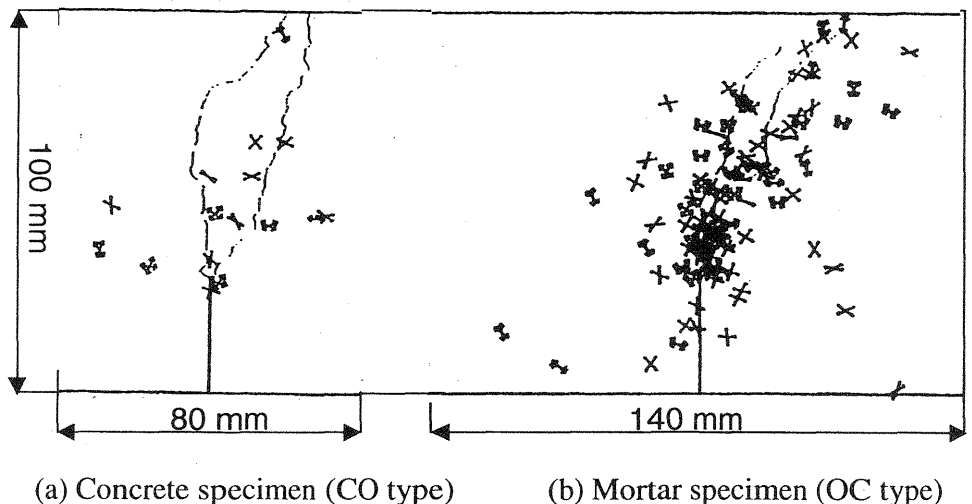


Fig. 3 Results of crack kinematics by the post-SiGMA

5.2 AE activity in the fracture process zone

AE counts observed on one channel for two specimens are given in Fig. 4. Load-CMOD (load-crack mouth opening displacement) curves are also shown in these figures. High AE activities are found right after the peak load in the CO type specimen of concrete, while AE activities gradually increase in the OC type specimen of mortar. This implies that cracks extend abruptly after the load reaches the peak in CO type specimens (see

Fig. 4a), but in OC-type specimen (see Fig. 4b) they continuously extend right from the beginning of loading. Because crack extension is arrested at aggregate inclusions, AE activities are observed intermittently in concrete. In mode-I cracking, high AE activities reflect the notch sensitivity of LEFM, even though the fracture process zone is formed ahead of the notch.

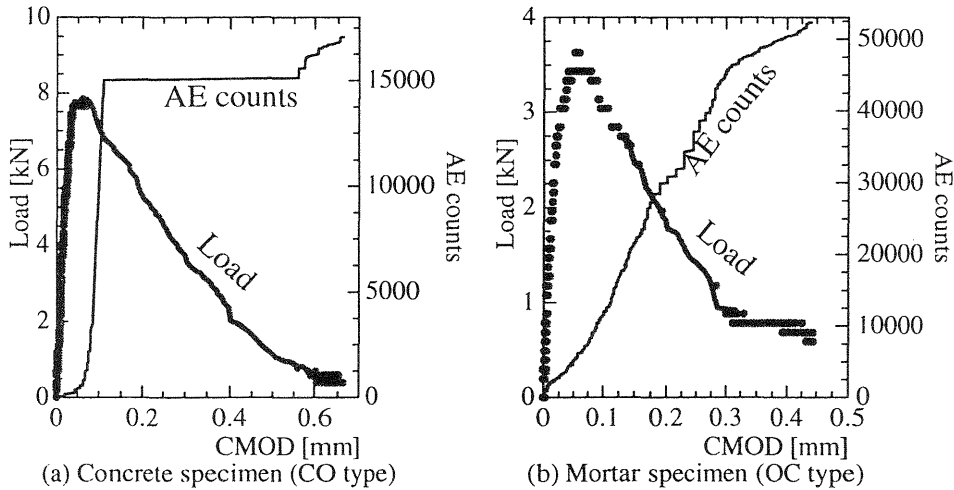


Fig. 4 Relation between CMOD, Load and AE Counts

5.3 Stress intensity factors and shear ratio

In order to classify the crack type, the shear ratio was applied (Ohtsu, 1995). The classification is based on the decomposition of eigenvalues of the moment tensor analysis in the SiGMA procedure. Here, not all AE signals could be successfully analyzed, only 10%-20% of the total AE signals could be analyzed. After the post analysis, the number of reliable solutions was so small so that the normalized stress intensity factors were calculated for all SiGMA solutions. Relations between the shear ratio and the normalized stress intensity factors of two specimens are plotted in Fig. 5. Here, the normalized stress intensity factors are estimated by only the absolute values. These figures, indicated that AE events for which the shear ratios are less than 40% obviously are associated to the larger K_{I}^* values. In contrast, K_{II}^* is dominant in AE events for which the shear ratios are larger than 60%. In the region between 40% and 60%, a mix-up of dominated K_{I}^* and K_{II}^* values is observed. This implies that the criterion for crack type classification based on the shear ratio in the SiGMA procedure is in reasonable agreement with the dominant mode of the stress intensity factors.

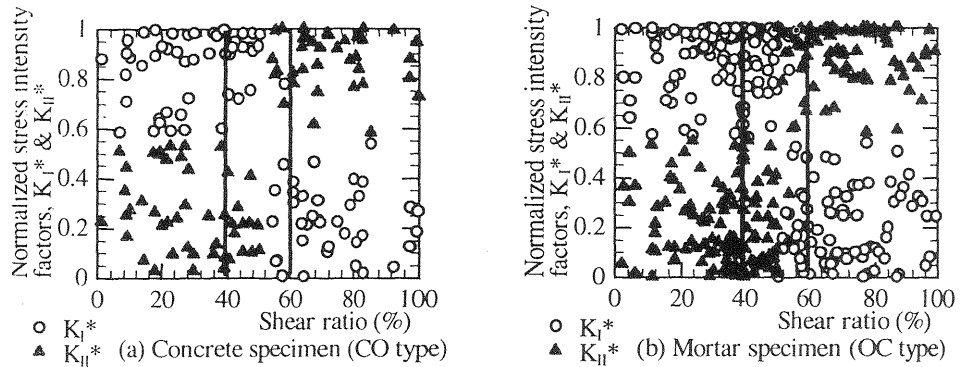


Fig. 5 Shear ratio versus normalized stress intensity factors

5.4 Estimation of the normalized stress intensity factors

When estimating the normalized stress intensity factors from eigenvectors of moment tensor components, one is confronted with two problems. The first pertains to the identification of the vectors l and n , because the two eigenvectors \bar{e}_1 and \bar{e}_3 could be determined alternately. The other problem concerns the definition of the normal vector n^0 to the pre-existing crack, in order to compute $\cos \theta = n^0 \cdot n^*$. In the present analysis, K_I/K_{II} values for the two vectors were determined, and then the vector which provided the larger K_I/K_{II} value, was designated the vector n^* . The normal vector n^0 was defined as the normal vector to the notch of the specimen. This implies that the normalized stress intensity factors were always calculated in respect to the notch of the specimen. Thus the effect of successive crack extension was not taken into consideration.

The normal components, $K_I^* = K_I/K_{IC}$ are plotted against the shear components, $K_{II}^* = K_{II}/K_{IC}$. Results of the CO type specimen of concrete and the OC type specimen of mortar are given in Fig. 6. The theoretical curve is obtained from Eq. 5 and 6, varying the angle θ . Some of the normalized stress intensity factors obtained were not coincident with the theoretical curve, probably due to the mis-identification of vector n^* . Consequently, only the normalized stress intensity factors which are coincident with the theoretical curve are plotted. It is realized that the normalized stress intensity factors under mixed-mode crack extension are reasonably estimated from the AE-SiGMA procedure. According to the figures, AE sources of which the normalized stress intensity factors K_I^* are larger than 0.6 are classified as tensile cracks, while those of which K_{II}^* are larger than 0.6 are classified as shear cracks. Although Eqs. 3 and 4 are based on only the critical value, K_{IC} , both types of cracks are identified. It implies that crack nucleation is macroscopically governed by mode I, whereas both types of mode I and mode II cracks are observed microscopically.

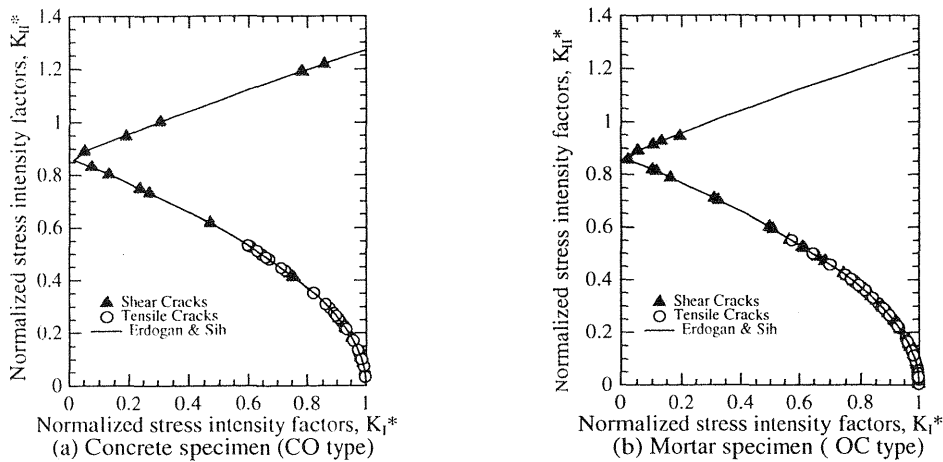


Fig. 6 Normalized stress intensity factors, K_I^* versus K_{II}^*

6 Conclusion

The direction of crack motion can be determined from the SiGMA procedure for crack extension. Based on the maximum circumferential stress crack initiation concept, normalized stress intensity factors $K_I^* = K_I/K_{IC}$ and $K_{II}^* = K_{II}/K_{IC}$ are estimated from tests of notched beams. Conclusions are summarized as follow:

- (1) A procedure to estimate the normalized stress intensity factors from the eigenvectors of the moment tensors is theoretically derived.
- (2) High AE activities right after the peak load are observed in the CO type specimen made of concrete, whereas continuous AE activities are observed in the OC type specimen fabricated of mortar. This reflects a crack-arresting effect due to aggregate inclusions in concrete.
- (3) AE sources are analyzed by the SiGMA procedure. Crack locations, crack types and crack orientations are determined. For these sources, normalized stress intensity factors are estimated. It is confirmed that the classification of the crack type based on the shear ratio is reasonably performed with respect to the dominant mode of the normalized stress intensity factors.
- (4) The relation between the normalized stress intensity factors K_I^* and K_{II}^* is investigated. AE sources of which the normalized stress intensity factors are coincident with the theoretical curve are selected. It is found that AE sources of K_I^* larger than 0.6 are classified as tensile cracks, while those of K_{II}^* larger than 0.6 are classified as shear cracks. Although the direction of the maximum circumferential stress is based on the critical values of K_{IC} , both types of cracks are identified. This is

implies that crack extension is macroscopically governed by the mode I, while both types of mode I and mode II are observed microscopically.

7 References

- Chahrour, A. H., Ohtsu, M. (1994) Crack growth prediction in scaled down model of concrete gravity dam, **Theoretical & Applied Fracture Mechanics**, 21, 29-40.
- Erdogan, F., Sih, G.C. (1963) On the crack extension in plates under plane loading and transverse shear, **J. of Basic Engineering**, ASME., 85, 519-527.
- Griffith, A. A. (1920) The phenomena of rupture and flow in solids, **Philosophical Transactions of the Royal Society of London**, Ser. A, Mathematical and Physical Sciences, 221, 163-198.
- Irwin, G. R. (1958) Fracture, **Encyclopedia of Physics**, Springer Berlin, 6, 551-590.
- Kaplan, M. F. (1961) Crack Propagation and the fracture of concrete, **ACI Journal**, 58(5), 591-610.
- Kim, K. Y., Sachse, W. (1984) Characterization of AE signals from indentation cracks in glass, **Progress in Acoustic Emission II**, JSNDI, 163-172.
- Ohtsu, M., Ono, K. (1984) A generalized theory of acoustic emission and Green's functions in half space, **J. of Acoustic Emission**, 3(1), 27-40.
- Ohtsu, M. (1991) Simplified moment tensor analysis and unified Decomposition of AE source, **J. of Geophysical Research**, 96(B4), 6211-6221.
- Ohtsu, M. (1995) Acoustic emission theory for moment tensor analysis, **Research on Non-Destructive Evaluation**, 6, 169-184.
- Suaris, W., van Mier, J. G. M. (1995) Acoustic emission source characterization in concrete under biaxial loading, **Material & Structures**, 28, 444-449.